DOI: 10.18721/JPM.13202
УДК 538.91

THE EFFICIENCY OF SOLAR ENERGY CONVERSION BY THE CdS/*por*-Si/*p*-Si HETEROSTRUCTURE: THE DOPANT EFFECT

V.V. Tregulov

Ryazan State University named for S. Yesenin, Ryazan, Russian Federation

In this paper, the effect of the distribution profile of the doping acceptor impurity concentration in the base region of the CdS/*por*-Si/*p*-Si heterostructure on the efficiency of solar energy conversion parameters has been studied. It was established that the solar energy conversion efficiency depended on the degree of a doping acceptor impurity depletion of the near-surface *p*-Si layer in the *por*-Si/*p*-Si heterojunction. The distribution profile of the impurity concentration in this space is formed during the growth of a porous silicon layer. This profile is controlled through changing the technological parameters of the process of a porous film growing: the current density and the duration time of the electrochemical etching. A gain in the conversion efficiency of solar energy was explained by an increase in the penetration depth of the electric field into the base region due to formation of a certain type of the impurity concentration distribution profile. In the final, this profile promotes the rapid carry-away of charge carriers generated by the light from the base region. This carry-away occurs before the carrier recombination moment involving traps.

Keywords: porous silicon, heterojunction, photovoltaic converter, solar cell, capacitance–voltage characteristic

Citation: Tregulov V.V. The efficiency of solar energy conversion by the CdS/*por*-Si/*p*-Si heterostructure: the dopant effect, St. Petersburg Polytechnical State University Journal. Physics and Mathematics. 13 (2) (2020) 17–26. DOI: 10.18721/JPM.13202

This is an open access article under the CC BY-NC 4.0 license (https://creativecommons.org/licenses/by-nc/4.0/)

ВЛИЯНИЕ ЛЕГИРУЮЩЕЙ ПРИМЕСИ НА ЭФФЕКТИВНОСТЬ ПРЕОБРАЗОВАНИЯ СОЛНЕЧНОЙ ЭНЕРГИИ ГЕТЕРОСТРУКТУРОЙ CdS/*por*-Si/*p*-Si

В.В. Трегулов

Рязанский государственный университет имени С.А. Есенина,
г. Рязань, Российская Федерация

В работе исследуется влияние профиля распределения концентрации легирующей акцепторной примеси в базовой области гетероструктуры CdS/*por*-Si/*p*-Si на параметры, характеризующие эффективность преобразования солнечной энергии. Установлено, что указанная эффективность зависит от степени обеднения легирующей акцепторной примесью приповерхностного слоя дырочного кремния (*p*-Si), входящего в структуру гетероперехода *por*-Si/*p*-Si. Профиль распределения концентрации примеси в данной области формируется в ходе роста слоя пористого кремния. Управление характером профиля распределения осуществляется через изменение технологических параметров процесса роста пористой пленки: плотностью тока и длительностью электрохимического травления. Повышение эффективности преобразования солнечной энергии объясняется увеличением глубины проникновения электрического поля внутрь базовой области за счет формирования определенного вида профиля распределения концентрации примеси. В конечном итоге вид профиля способствует быстрому выносу из базовой области носителей заряда, генерируемых светом; вынос происходит до момента рекомбинации носителей при участии ловушек.

Ключевые слова: пористый кремний, гетеропереход, фотовольтаический преобразователь, солнечный элемент, вольт-фарадная характеристика

Ссылка при цитировании: Трегулов В.В. Влияние легирующей примеси на эффективность преобразования солнечной энергии гетероструктурой CdS/*por*-Si/*p*-Si // Научно-технические ведомости СПбГПУ. Физико-математические науки. 2020. Т. 13. № 2. С. 17–26. DOI: 10.18721/JPM.13202

Статья открытого доступа, распространяемая по лицензии CC BY-NC 4.0 (https://creative-commons.org/licenses/by-nc/4.0/)

Introduction

Currently quite a lot of interest is being shown in the study of the solar photovoltaic converter based on the CdS/*por*-Si/*p*-Si heterostructure [1, 2]. The CdS film plays the role of an optical window and significantly expands the spectral sensitivity region of the photovoltaic converter [3, 4]. The *por*-Si layer is a buffer that reduces the mechanical stresses arising between the silicon substrate and the CdS film due to the difference in the lattice constants (about 7 %) [4, 5]. In addition, the *por*-Si film reduces the reflectivity of the front surface of the CdS/*por*-Si/*p*-Si photovoltaic converter [4]. An important advantage of the CdS/*por*-Si/*p*-Si heterostructure is the absence of the need to form a $p - n$ junction by diffusion in *p*-Si. This will reduce the complexity of the manufacturing process of the photovoltaic cells and its cost, which is important in mass production. Thus the CdS/*por*-Si/*p*-Si heterostructure is relevant for use in solar energy.

In this regard the urgent task is to develop solutions aimed at increasing the efficiency of the CdS/*por*-Si/*p*-Si heterostructure as a solar energy converter.

One way to solve this problem is to increase the collection efficiency of charge carriers generated by light in the absorbing region of the photovoltaic converter. It is well known that the separation of photogenerated charge carriers occurs under the influence of an electric field concentrated in the space charge region (SCR) of the photovoltaic converter barrier layer (in our case, a heterojunction). Due to the strong electric field the carriers are removed from the SCR before they have time to recombine through the participation of traps [6]. Thus, to increase the efficiency of carrier separation, it is advisable to create conditions for expanding the region located inside the absorbing layer in which the strongest electric field is concentrated. For this purpose, it is desirable to set up a concentration gradient of the dopant in the surface region of the absorbing layer of the photovoltaic converter [6, 7]. According to Ref. [6] these methods lead to an increase in the efficiency of solar energy conversion due to an increase in open circuit voltage and short circuit current.

The experimental samples studied in this work are similar to the CdS/*por*-Si/*p*-Si heterostructure investigated in Ref. [8] where it was shown the largest contribution to the photocurrent to make by charge carriers absorbed in *p*-Si. In addition, the SCR of the studied heterostructure was almost completely concentrated in the surface region of the *p*-Si heterojunction of the *por*-Si/*p*-Si. Thus, the base region of the CdS/*por*-Si/*p*-Si heterostructure is located in the near-surface *p*-Si layer close to the *por*-Si/*p*-Si heterojunction. The charge carriers generated by light are separated by the electric field of the *por*-Si/*p*-Si heterojunction [8].

The high-frequency capacitance – voltage ($C - V$) characteristics of *por*-Si/*p*-Si structures were studied, and in this case the *por*-Si film was formed by anodic electrochemical etching at various values of the etching duration t_{et} and the anode current density J_{et} [9, 10]. It was found that with an increase in J_{et} and t_{et} in silicon, a depleted dopant region was formed near the *por*-Si/Si heterojunction.

In this paper, the influence of the distribution profile of the acceptor dopant concentration on the solar energy conversion efficiency for the absorbing *p*-Si layer of the CdS/*por*-Si/*p*-Si heterostructure has been investigated.

In order to control this distribution profile, a *por*-Si film of the samples under investigation was

Table

Information on the experimental samples

No.	J_{et}, mA/cm^2	t_{et}, min	U_{oc}, mV	J_{sc}, mA/cm^2	FF, arb.unit.	η, %	N_t, cm^{-3}
1	10	12	365	12.1	0.6	3.4	$4.2 \cdot 10^{13}$
2	18	10	487	16.5	0.7	5.7	$9.7 \cdot 10^{13}$
3	30	7	475	14.2	0.7	4.6	$2.0 \cdot 10^{14}$
4	45	5	270	9.6	0.6	1.6	$2.3 \cdot 10^{14}$

Symbols: J_{et} is the anode current density, t_{et} is the etching duration,
U_{oc} is the open circuit voltage, J_{sc} is the short-circuit current density,
FF is the filling factor of the current-voltage characteristic, η is the efficiency,
N_t is the concentration of traps.

formed at different values of the etching duration t_{et} and the anode current density J_{et}.

The technology of manufacturing experimental samples

For the preparation of experimental CdS/*por*-Si/*p*-Si samples the *p*-type single-crystal silicon wafers with a specific resistance of 1 Ohm·cm doped with boron and a surface orientation of (100) were used. The concentration of the doping acceptor impurity in the silicon wafers was $1.5 \cdot 10^{16}$ cm^{-3}. The *por*-Si film was made by the technique of anodic electrochemical etching in the galvanostatic mode. An electrolyte consisting of HF and C_2H_5OH in a ratio of 1:1 was used. Several samples were made with different values of J_{et} and t_{et} (see Table). The time t_{et} values for the samples were chosen so that the *por*-Si film thickness at different J_{et} values was approximately the same. After the *por*-Si film was grown, the surface of the samples was etched in an aqueous HF solution (10 %) for 10 min. The *por*-Si film thickness for all samples was 2.2 ± 0.3 µm.

A CdS film was formed on the surface of a *por*-Si layer by the method of chemical bath deposition (from aqueous solutions). A $CdCl_2$ solution with a concentration of 0.44 M was used as a source of cadmium ions. An N_2H_4CS (thiourea) solution with a concentration of 0.22 M was used as a source of sulfur ions. A concentrated aqueous NH_4OH (ammonia) solution was used as a complexing agent. At first, an ammonia solution was added to the $CdCl_2$ one until the precipitate completely dissolved, then the same volume of an aqueous thiourea solution was added to the resulting solution. The temperature of the solution was brought to 90° C, substrates with a *por*-Si film were immersed in it, and a CdS film was grown for 20 min. The CdS layer on the back side of *p*-Si was completely etched with a 30% HCl solution. Samples were washed with distilled water and dried in the oven. For all samples, the CdS film thickness was 1.8 ± 0.2 µm.

For electrical measurements, ohmic contacts were formed on opposite surfaces of the sample to the *p*-Si substrate and the CdS film by soldering indium.

The used investigation technique

In order to study the distribution profile of the dopant concentration in the base region of the structure given above, the $C-V$ characteristics were measured at a frequency of 1 MHz at a reverse bias. The reverse bias corresponds to the application of a positive value of the constant bias voltage U to the contact on the CdS surface and negative U to the contact on the *p*-Si. The measurements of the samples were carried out using an E7-20 digital immitance meter (MNIPI, Belarus) at a temperature of 300 K. It is known that the high-frequency $C-V$ characteristic $C(U)$ measured at reverse bias reflects the dependence of the capacitance barrier component on the applied voltage and allows one to determine the impurity concentration in the base region of the studied semiconductor structure:

$$N_b = \frac{2}{q\varepsilon\varepsilon_0 S^2} \cdot \left(\frac{dC(U)^{-2}}{dU} \right)^{-1}, \quad (1)$$

where q is the electron charge, ε is the dielectric constant of the semiconductor material of the base region of the studied heterostructure (silicon), ε_0 is the vacuum dielectric constant, S is the sample area [7].

The value of the x coordinate is calculated by the formula [7]:

$$x = \frac{\varepsilon\varepsilon_0 S}{C(U)}. \quad (2)$$

The combined use of formulas (1) and (2) allows us to calculate the distribution profile of the concentration of the dopant $N_b(x)$ in the base region of the investigated semiconductor structure.

The calculation of the distribution profile of the electric field in the SCR of the studied samples was carried out as follows [7]:

$$E(x) = -\frac{q}{\varepsilon\varepsilon_0} N_b(x) \cdot (x - W), \quad (3)$$

where W is the width of the SCR.

The main characteristics of solar photovoltaic converters with heterojunctions are significantly affected by surface states, and also traps with energy levels located in the bulk of the base region [6]. In order to obtain information about traps, we studied the $C - V$ hysteresis measured at a frequency of 1 MHz in the region of reverse biases.

Despite the fact that at high frequencies the charge in traps with deep energy levels does not have time to follow the measuring signal, it affects the value of W and the value of the high-frequency capacitance [11]. To evaluate the influence of traps, one can compare the $C - V$ characteristic, measured with the forward bias of a constant bias voltage from 0 to a certain limiting value U_m ($C_{in}(U)$), and measured with a reverse scan from U_m to 0 ($C_{out}(U)$). In the absence of traps, the $C_{in}(U)$ and $C_{out}(U)$ curves should coincide completely. In the presence of traps a hysteresis phenomenon is observed – the $C_{in}(U)$, and $C_{out}(U)$ curves differ [12]. Thus, by analyzing the width of the hysteresis band formed by the $C_{in}(U)$ and $C_{out}(U)$ curves, we can obtain information about traps in the SCR.

The value of the barrier capacitance is determined by the ratio of the charge increment in the SCR to the magnitude of the voltage change [7]:

$$C = \frac{dQ}{dU}. \quad (4)$$

Hence, the charge Q concentrated in the SCR, when the constant bias voltage changes from U_1 to U_2, can be expressed as follows:

$$Q = \int_{U_1}^{U_2} C(U)\, dU. \quad (5)$$

On the other hand, the charge Q is determined by the volume concentrations of the dopant N_b and of the traps N_t, as well as the SCR thickness W:

$$Q = q(N_b + N_t)WS. \quad (6)$$

Given the hysteresis of the $C - V$ curves and using Eqs. (5) and (6), for the concentration of traps we can write the following expression:

$$N_t = \frac{1}{qWS} \int_0^{U_m} \left| C_{in}(U) - C_{out}(U) \right| dU, \quad (7)$$

where U_m is the limiting value of the constant bias voltage to which the constant bias voltage U is scanned.

To evaluate the efficiency of solar energy conversion by CdS/*por*-Si/*p*-Si samples, we measured the open circuit voltage U_{oc}, short-circuit current density J_{sc}, filling factor of the current – voltage characteristic FF and efficiency η under illumination under AM1.5.

Experimental results

Capacitance – voltage characteristics of the samples under study, measured in the region of reverse biases, are shown in Fig. 1 in the form of the dependence $(C/S)^{-2} = f(U)$. For sample No. 1, the graph in Fig. 1 is close to a straight

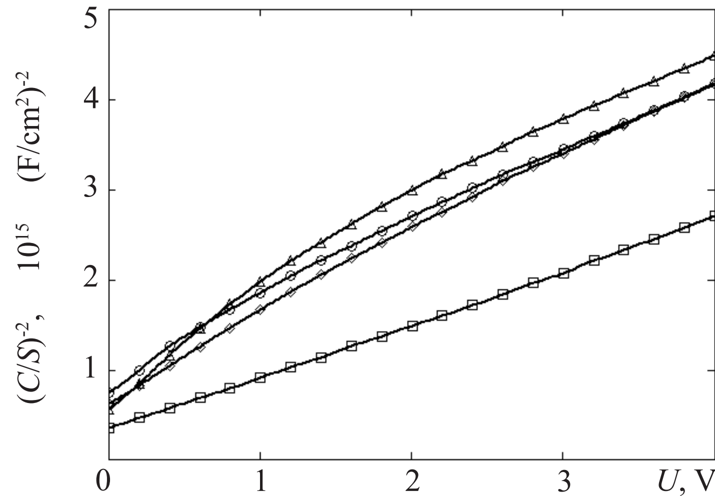

Fig. 1. Capacitance – voltage characteristics of samples No. 1 (□), No. 2 (◊), No. 3 (○), No. 4 (Δ), measured at a frequency of 1 MHz with reverse bias; S is the sample area

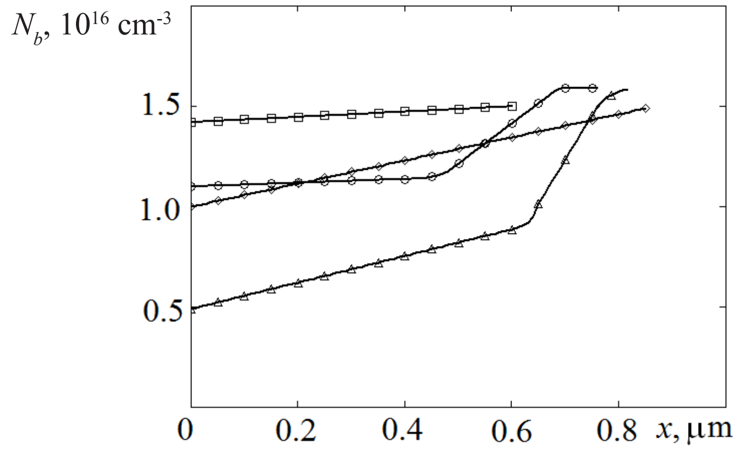

Fig. 2. Distribution profiles of the concentration of acceptor impurities in the base region of samples No. 1 (□), No. 2 (◊), No. 3 (○), No. 4 (Δ)

line. For samples No. 2 – No. 4, the dependence $(C/S)^{-2} = f(U)$ noticeably deviates from the linear one, which indicates the presence of an impurity concentration gradient in the base region (see Fig. 1).

The profiles of the distribution dopant concentration $N_b(x)$ in the surface layer of the base region of the samples under study, calculated by Eqs. (1) and (2), are shown in Fig. 2. For sample No.1, the N_b value varies slightly with the x coordinate and is close to the acceptor impurity concentration ($1.5 \cdot 10^{16}$ cm^{-3}) in silicon wafers used as a substrate for the manufacture of the samples. For sample No. 2, the value N_b increases linearly with increasing x to a value close to $1.5 \cdot 10^{16}$ cm^{-3}. Samples No. 3 and No. 4 are characterized by a more complex dependence $N_b(x)$. Thus, for samples No. 2 – No. 4 an acceptor impurity is depleted in the surface layer of the base region directly adjacent to the *por*-Si/*p*-Si heterojunction. With an increase in x the value of N_b tends to a value close to $1.5 \cdot 10^{16}$ cm^{-3}.

The electric field distribution profile $E(x)$ for the studied samples calculated by Eq. (3) is presented in Fig. 3. Sample No. 1 exhibits a linear dependence $E(x)$ with a sharp heterojunction. The maximum value of E for samples No. 1 – No. 3 practically coincides. The region width bounded by the dependence $E(x)$ is maximum value for sample No. 2.

In order to estimate the traps concentration N_t the C – V characteristics of the samples were

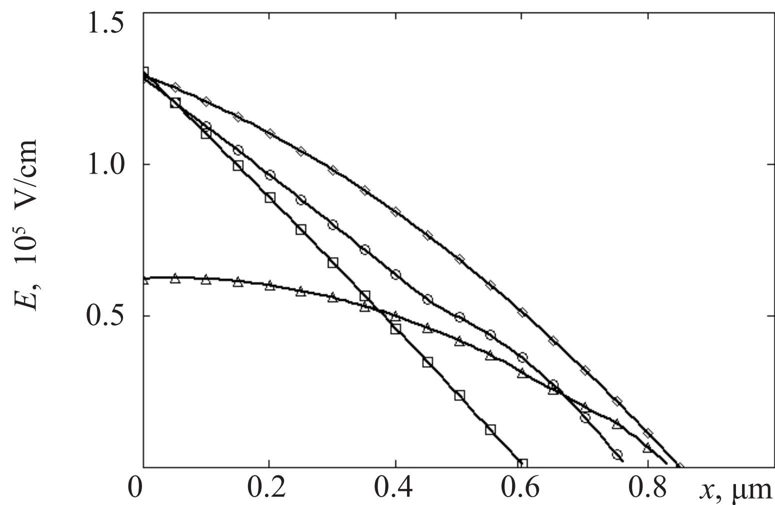

Fig. 3. The distribution profiles of the electric field in the base region of samples No. 1 (□), No. 2 (◊), No. 3 (○), No. 4 (Δ)

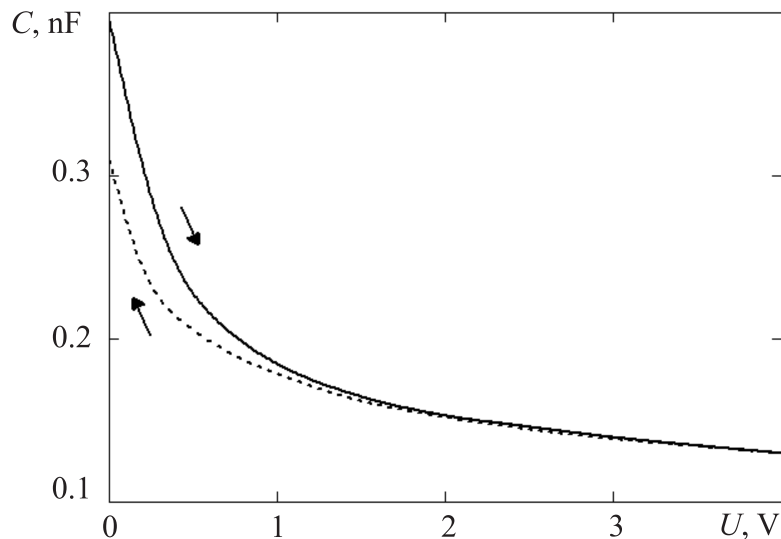

Fig. 4. Capacitance – voltage characteristics of sample No. 2 for a forward sweep of a constant bias voltage (solid line) and reverse (dashed line)

measured at direct $C_{in}(U)$ and reverse $C_{out}(U)$ scans of a constant bias voltage U in the range 0 – 4 V. For all the samples studied the behavior of the $C_{in}(U)$ and $C_{out}(U)$ is almost identical. The curves $C_{in}(U)$ and $C_{out}(U)$ for sample No. 2 are shown in Fig. 4. The $C_{in}(U)$ and $C_{out}(U)$ curves noticeably differ in the range of U values from 0 to 2 V; for $U > 2$ V this difference practically disappears (see Fig. 4). This behavior of the curves in Fig. 4 can be explained by a more noticeable effect on the barrier capacitance of traps localized at the *por*-Si/*p*-Si heterojunction (surface states) as compared to traps located in the bulk of the base region of the samples.

The values of U_{oc}, J_{sc}, FF and η, characterizing the efficiency of solar energy conversion of the studied samples, are presented in Table. The highest efficiency of solar energy conversion is characterized by sample No. 2; sample No. 3 is close to it; sample No. 4 has the lowest conversion efficiency compared to samples No. 1 – No. 3 (see Table).

Discussion of the experimental results

The efficiency of a solar photovoltaic converter with a heterojunction is significantly affected by surface states and traps located in the volume of

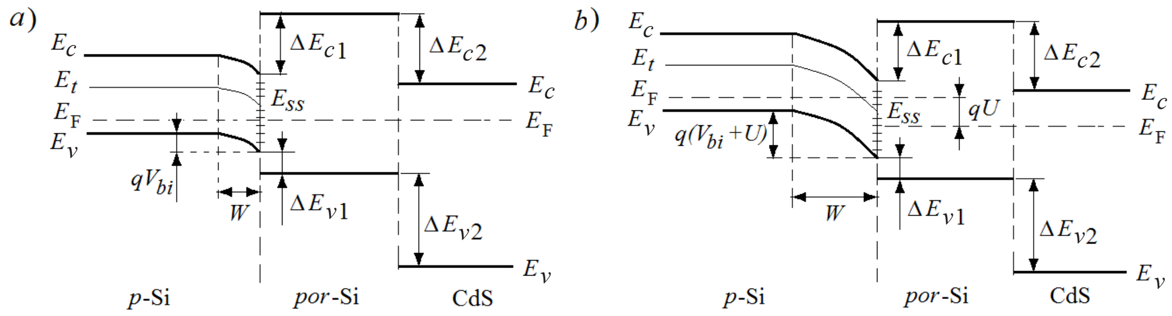

Fig. 5. The band diagram of the CdS/*por*-Si/*p*-Si heterostructure at $U = 0$ V (*a*) and for some value of reverse bias U (*b*); see explanations in the text

the absorbing region [6]. However, it is impossible to draw an unambiguous conclusion about the effect of the concentration N_t on the solar energy conversion efficiency of experimental samples from the Table. So, sample No. 4 has significantly lower values of U_{oc}, J_{sc}, and η compared to sample No. 3. Moreover, for these samples the value of N_t changes slightly. Sample No. 2, characterized by the highest conversion efficiency η, has an N_t value close to samples No. 3 and No. 4. At the same time sample No. 1 which occupies an intermediate place between samples No. 3 and No. 4 in terms of conversion efficiency η, is characterized by the lowest N_t value of all the samples studied. Moreover, the N_t value of sample No. 1, is significantly less than for the remaining samples. Thus, the value of N_t does not have a decisive influence on the parameters characterizing the conversion efficiency of the studied samples.

An analysis of the hysteresis for the $C - V$ characteristics (see Fig. 4) shows that the capacitance decreases upon reverse sweep U. In Ref. [11] the decrease in the SCR capacitance was explained by the emptying of the traps of minority charge carriers. This situation can be illustrated by zone diagrams in Fig. 5.

The SCR of a width W is almost completely concentrated in the surface *p*-Si layer near the *por*-Si/*p*-Si heterojunction. At this heterojunction, surface states characterized by energy levels of E_{ss} are localized, and traps with energy levels of E_t can also be contained in the bulk of the *p*-Si base region (see Fig. 5). It was shown [8], that the current flow mechanisms in the studied CdS/*por*-Si/*p*-Si heterostructure are determined by the traps with activation energies occupying a wide range of values. For the purpose of simplification, only one volumetric energy level E_t is shown in Fig. 5. At $U = 0$ V (see Fig. 5,*a*), the band bending in the *p*-Si region is determined by the value of the diffusion potential V_{bi}. In this case the energy levels of the E_t and E_{ss} traps located within the SCR of the *por*-Si/*p*-Si heterojunction are filled with charge carriers if they are below the Fermi level E_F and emptied if they are above E_F.

In the reverse bias (see Fig. 5,*b*), the band bending in the SCR increases by the value of the applied voltage U, the energy levels of the traps below E_F are filling with carriers. Upon subsequent change in the scanning direction U to 0 V the bending of the zones decreases, and a transition to the conditions shown in Fig. 5,*a* takes place. This is accompanied by the depletion of the energy levels of the E_t and E_{ss} traps. Moreover, the dominant contribution to the relaxation process is made by the energy levels of minority carrier traps in the *p*-Si layer.

The most probable cause of the observed differences in the efficiency parameters of the studied samples (see Table) may be the difference in the character of the dependence $E(x)$ in the SCR of the base region of the *por*-Si/*p*-Si heterojunction (see Fig. 3). In turn, the form of the dependence $E(x)$ is determined by the distribution dopant concentration profile $N_b(x)$ (see Fig. 2). Referring to Figs. 2 and 3, depletion of the *p*-Si surface region by an acceptor impurity for samples No. 2 and No. 3 leads to a noticeable extension of the $E(x)$ curves towards an increase in x as compared to that of sample No. 1, for which the N_b value weakly depends on x within

the SCR. Moreover, the efficiencies of samples No. 2 and 3 are significantly higher as compared to that of sample No. 1. The near-surface layer of the *p*-Si region of sample No. 4 is more depleted in acceptor impurity than those of samples No. 1 – No. 3 (see Fig. 2). As a result, the electric field inside the SCR is noticeably lower for sample No. 4 than those for the remaining samples (see Fig. 3). Sample No. 4 exhibits the lowest conversion efficiency of solar energy as compared to those for the rest of the studied samples.

Thus, an increase in the conversion efficiency of solar energy of the studied samples can be explained by an increase in the penetration depth of a strong electric field into the base region. The charge carriers generated by the light inside this region are carried away by the electric field before they have time to recombine through the participation of traps. Thus, the depletion of the doping impurity in the near-surface *p*-Si layer which is in the immediate vicinity of the *por*-Si/*p*-Si heterojunction, is an aid to the expansion of the region in which the strongest electric field is concentrated. At the same time an increase in the depletion of the base region with an alloying impurity observed for sample No. 4 leads to a decrease in the electric field strength (see Fig. 3) and a decrease in the efficiency of solar energy conversion (see Table).

The depletion of the *p*-Si surface region occurs during the formation of a *por*-Si film. One of the causes of depletion may be the partial etching of impurity atoms from the surface of silicon crystallites during the formation of a porous layer [13]. Another cause of the depletion may be a partial compensation of the main dopant by defects, including those having deep energy levels localized on the surface of silicon crystallites [9, 13].

Numerous studies have shown that *por*-Si films formed on single-crystal silicon substrates are complexly structured [14 – 16]. The *por*-Si film is formed by silicon crystallites separated by pores. The average crystallite diameter increases as it moves from the outer surface of the *por*-Si film to the single-crystal substrate [16]. Thus, a clearly defined boundary between the porous film and the single crystal substrate may be absent. As a result, the *por*-Si/*p*-Si heterojunctions of the samples studied in this work can be located inside the largest silicon crystallites in the lower region of the *por*-Si film. The states localized on the crystallite surface can contribute to partial compensation of the acceptor dopant in the surface layer of the base region of the samples under study.

Summary

The relationship between the distribution profile of the dopant acceptor impurity in the base region of the CdS/*por*-Si/*p*-Si heterostructure and the solar energy conversion efficiency parameters has been established. It was shown that the conversion efficiency depends on the degree of depletion of the *p*-Si surface layer doping with an acceptor impurity located in the immediate vicinity of the *por*-Si/*p*-Si heterojunction. The formation of this depletion region occurs as a result of a *por*-Si film growing. By changing the main parameters of the *por*-Si growth process (t_{et} and J_{et}) one can control the impurity distribution profile and the efficiency of solar energy conversion. Thus, in order to increase its efficiency, one of the directions of optimizing the technology of the solar photovoltaic converter based on the CdS/*por*-Si/*p*-Si heterostructure is the selection of t_{et} and J_{et} parameters for *por*-Si film growing. An important advantage is a forming of the depleted region not requiring a separate technological operation. The concentration distribution profile is formed in the process of growing the *por*-Si layer. In production conditions this will reduce the cost of manufacturing a photovoltaic converter.

The obtained data can be useful in the development of solar photovoltaic converters and optical sensors based on the CdS/*por*-Si/*p*-Si heterostructure.

REFERENCES

1. **Hasoon S.A., Ibrahim I.M., Raad M.S., et al.,** Fabrication of nanostructure CdS thin film on nanocrystalline porous silicon, International Journal of Current Engineering and Technology. 4 (2) (2014) 594–601.

2. **Jafarov M.A., Nasirov E.F., Jahangirova**

S.A., Nano-CdS/porous silicon heterojunction for solar cell, International Journal of Scientific and Engineering Research. 6 (7) (2015) 849–853.

3. **Sharma B.L., Purohit R.K.,** Semiconductor heterojunctions, Pergamon Press, Oxford, New York, 1974.

4. **Mamedov H.M., Kukevecz A., Konya Z., et al.,** Electrical and photoelectrical characteristics of *c*-Si/*porous*-Si/CdS heterojunctions, Russian Physics Journal. 61 (9) (2019) 1660–1666.

5. **Eesa M.W., Abdullah M.M.,** Porous silicon effect on the performance of CdS nanoparticles photodetector, International Journal of Current Engineering and Technology. 4 (6) (2016) 1372–1376.

6. **Fahrenbuch A.L., Bube R.H.,** Photovoltaic solar energy conversion, Fundamentals of solar cells, Academic Press, New York, 1983.

7. **Sze S.M.,** Physics of semiconductor devices: Second Ed., John Wiley and Sons, New York, Chichester, Brisbane, Toronto, Singapore, 1981.

8. **Tregulov V.V., Litvinov V.G., Ermachikhin A.V.,** Study of current flow mechanisms in a CdS/*por*-Si/*p*-Si heterostructure, Semiconductors. 52 (7) (2018) 891–896.

9. **Timokhov D.F., Timokhov F.P.,** Determination of structure parameters of porous silicon by the photoelectric method, Journal of Physical Studies. 8 (2) (2004) 173–177.

10. **Hadi H.A., Abood T.H., Mohi A.T., Karim M.S.,** Impact of the etching time and current density on capacitance-voltage characteristics of *p*-type of porous silicon, World Scientific News. 67 (2) (2017) 149–160.

11. **Berman L.S., Lebedev A.A.,** Emkostnaya spektroskopiya glubokih centrov v poluprovodnikah [Deep-center capacity spectroscopy in semiconductors] Nauka, Leningrad, 1981 (In Russian).

12. **Voitsekhovskii A.V., Nesmelov S.N., Dzyadukh S.M.,** Electrical characterizations of MIS structures based on variable-gap *n*(*p*)-HgCdTe grown by MBE on Si(013) substrates, Infrared Physics and Technology. 87 (December) (2017) 129–133.

13. **Zhang X.G.,** Electrochemistry of silicon and its oxide, Kluwer Academic Publishers, New York, Boston, Dordrecht, London, Moscow, 2004.

14. **Goryachev D.N., Belyakov L.V., Sreseli O.M.,** Formation of thick porous silicon layers with insufficient minority carrier concentration, Semiconductors. 38 (6) (2004) 712–716.

15. **Venger E.F., Gorbach T.Ya., Kirillova S.I., et al.,** Changes in properties of a porous silicon/silicon system during gradual etching off of the porous silicon layer, Semiconductors. 36 (3) (2002) 330–335.

16. **Melnik N.N., Tregulov V.V.,** Photoluminescence and Raman studies of the structure of a thick porous silicon film, Bulletin of the Lebedev Physics Institute. 42 (3) (2015) 77–80.

Received 20.03.2020, accepted 04.05.2020.

THE AUTHOR

TREGULOV Vadim V.

Ryazan State University named for S. Yesenin

46, Svobody St., Ryazan, 390000, Russian Federation

trww@yandex.ru

СПИСОК ЛИТЕРАТУРЫ

1. **Hasoon S.A., Ibrahim I.M., Raad M.S., Al-Haddad, Mahmood S.S.** Fabrication of nanostructure CdS thin film on nanocrystalline porous silicon // International Journal of Current Engineering and Technology. 2014. Vol. 4. No. 2. Pp. 594–601.

2. **Jafarov M.A., Nasirov E.F., Jahangirova S.A.** Nano-CdS/porous silicon heterojunction for solar cell // International Journal of Scientific and Engineering Research. 2015. Vol. 6. No. 7. Pp. 849–853.

3. **Шарма Б.Л., Пурохит Р.К.** Полупроводниковые гетеропереходы. Пер. с англ. М.: Сов. радио, 1979. 232 с.

4. **Мамедов Г.М., Кукевеч А., Коня З., Кордаш К., Шах С.И.** Электрические и фотоэлектрические характеристики гетеропереходов *c*-Si/пористый-Si/CdS // Известия высших учебных заведений. Физика. 2018. Т. 61. № 9. С. 96–101.

5. **Eesa M.W., Abdullah M.M.** Porous silicon effect on the performance of CdS nanoparticles photodetector // International Journal of Current Engineering and Technology. 2016. Vol. 4. No. 6. Pp. 1372–1376.

6. **Фаренбух А., Бьюб Р.** Солнечные элементы: теория и эксперимент. Пер. с англ. М.: Энергоатомиздат, 1987. 280 с.

7. **Зи С.М.** Физика полупроводниковых приборов: Пер. с англ. В 2 тт. Т. 1. М.: Мир, 1984. 456 с.

8. **Трегулов В.В., Литвинов В.Г., Ермачихин А.В.** Исследование механизмов токопрохождения в гетероструктуре CdS/*por*-Si/*p*-Si / Физика и техника полупроводников // 2018. Т. 52. № 7. С. 751–756.

9. **Timokhov D.F., Timokhov F.P.** Determination of structure parameters of porous silicon by the photoelectric method // Journal of Physical Studies. 2004. Vol. 8. No. 2. Pp. 173–177.

10. **Hadi H.A., Abood T.H., Mohi A.T., Karim M.S.** Impact of the etching time and current density on Capacitance–Voltage characteristics of *p*-type of porous silicon // World Scientific News. 2017. Vol. 67. No. 2. Pp. 149–160.

11. **Берман Л.С., Лебедев А.А.** Емкостная спектроскопия глубоких центров в полупроводниках. Л.: Наука, 1981. 176 с.

12. **Voitsekhovskii A.V., Nesmelov S.N., Dzyadukh S.M.** Electrical characterizations of MIS structures based on variable-gap *n*(*p*)-HgCdTe grown by MBE on Si(013) substrates // Infrared Physics and Technology. 2017. Vol. 87. December. Pp. 129–133.

13. **Zhang X.G.** Electrochemistry of silicon and its oxide. New York, Boston, Dordrecht, London, Moscow: Kluwer Academic Publishers, 2004. 510 p.

14. **Горячев Д.Н., Беляков Л.В., Сресели О.М.** Формирование толстых слоев пористого кремния при недостаточной концентрации неосновных носителей // Физика и техника полупроводников. 2004. Т. 38. № 6. С. 739–744.

15. **Венгер Е.Ф., Горбач Т.Я., Кириллова С.И., Примаченко В.Е., Чернобай В.А.** Изменение свойств системы пористый Si/Si при постепенном стравливании слоя пористого Si // Физика и техника полупроводников. 2002. Т. 36. № 3. С. 349–354.

16. **Мельник Н.Н., Трегулов В.В.** Исследование структуры толстой пленки пористого кремния методами фотолюминесценции и комбинационного рассеяния света // Краткие сообщения по физике ФИАН. Т. 42. № 3. 2015. С. 19–24.

Статья поступила в редакцию 20.03.2020, принята к публикации 04.05.2020.

СВЕДЕНИЯ ОБ АВТОРЕ

ТРЕГУЛОВ Вадим Викторович – *кандидат технических наук, доцент кафедры общей и теоретической физики и методики преподавания физики Рязанского государственного университета имени С.А. Есенина, г. Рязань, Российская Федерация.*

390000, Российская Федерация, г. Рязань, ул. Свободы, 46

trww@yandex.ru

© Санкт-Петербургский политехнический университет Петра Великого, 2020